Journal of Photochemistry and Photobiology B: Biology 139 (2014) 34–38

Contents lists available at ScienceDirect

Journal of Photochemistry and Photobiology B: Biology

journal homepage: www.elsevier.com/locate/jphotobiol

Highly sensitive imaging for ultra-weak photon emission from living organisms

Masaki Kobayashi *

Tohoku Institute of Technology, Sendai 982-8577, Japan

ARTICLE INFO

Article history:
Available online 1 December 2013

Keywords:
Ultra-weak photon emission
Biophoton
Imaging
CCD
Photon-counting
Reactive oxygen species

ABSTRACT

Spontaneous ultra-weak photon emissions (UPEs) are from living organisms. Often designated as biophoton emissions, they are associated with reactive oxygen species production. They have long been explored for use in the extraction of pathophysiological information of living bodies. Because of its potential non-invasiveness and because it is completely passive, it has been anticipated for application to human diagnosis. However, because of the weakness of its signal and the complexity of the mechanisms, practical applications of UPE and efforts have remained restricted.

Imaging of UPE is a powerful tool for the practical application of UPE. Furthermore, efforts to develop imaging technique have been made from the early period of UPE study. This report explains the history of UPE study, particularly describing the development of imaging technology and its application covering agriculture and medicine are reviewed. Furthermore, the issue of what was achieved and what is necessary for the additional advancement of UPE will be discussed for practical application.

1. Introduction

Ultra-weak photon emissions (UPEs) from living organisms, often designated as biophoton emissions, occur as widely known phenomena that are widely observed in living organisms. Although photon emissions are accompanied by biological functions, their intensity is extremely weak, typically 3–6 orders lower intensity than the threshold of human visual recognition. Photon emission originates via reactive oxygen species (ROS) generated under processes of biochemical reactions with normal metabolism and/or an abnormal state promoted by ROS. Intensity variations of UPE reflect metabolic activity or changes of balance between the ROS level and antioxidant capacity. The emissions can provide valuable information about the state of oxidative stress without invasion of a monitor. Actually, UPE has long been anticipated for use as a signal mediator carrying pathophysiological information. Because of its potential for non-invasiveness and complete passivity, it has attracted attention as offering an 'ultimate' methodology for the diagnosis of human illness. Although numerous phenomena of UPE have been described during the last half-century, the practical application of UPE has remained restricted because of the weakness of the signal and the complexity of its related mechanism. To characterize and extract information, the spectral, spatial, and other optical properties including photon statistics should be used in such a single-photon level. In Japan, Professor Inaba, a world pioneer in this field, and his biophoton projects have led research in this field since the 1970s. His work has achieved the development of various technologies for precise measurement while pursuing their mechanisms.

To identify the properties of UPE for extracting valuable information, visualization as two-dimensional (2D) images is necessary for non-invasive diagnosis. This paper presents a review of the techniques and systems developed for UPE imaging. Efforts to achieve UPE imaging have been undertaken from the mid-1980s. Characteristics of each technique and evaluation of experimentally obtained results indicating the feasibility of UPE imaging for practical applications are discussed with attention to applications in fields such as medicine, agriculture, and other bio-industries.

2. UPE imaging technology

In the history of UPE research, the first imaging was accomplished using an imaging system employing a 2D photon-counting tube. After that, to the present day, the scientific grade of charge-coupled-devices (CCDs) with cooling equipment has been generally used for UPE imaging. Here, these two types of imaging devices and imaging systems are reviewed, with evaluation of a lens system, which is a key device for UPE imaging.

2.1. Two-dimensional photon-counting imaging system

The development of a 2D photon-counting tube [1] comprising a uniform photocathode, a set of micro-channel plates (MCPs), and

* Tel.: +81 223053211; fax: +81 223053202.
E-mail address: masaki@tohtech.ac.jp

1011-1344/$ - see front matter © 2013 Elsevier B.V. All rights reserved.
http://dx.doi.org/10.1016/j.jphotobiol.2013.11.011

a position-sensitive-anode (also designated as a resistive anode or a position sensitive device) triggered the study of UPE imaging. An MCP is an electron multiplying device which conserves the spatial information of released photoelectrons from the photocathode. The position-sensitive-anode identifies an X–Y coordinate of a multiplied photoelectron-pulse from MCP through calculation. The pulses are accumulated as the number of events in the corresponding address on the frame memory in an image processor. Consequently, a photon-counting image is depicted with a gray-scale indication of the number of photoelectrons in each pixel. A schematic diagram of a typical 2D photon-counting tube is portrayed in Fig. 1.

The first image of UPE from a living organism was demonstrated using a germinating soybean, indicating intense emissions from the active area of mitosis [2]. The experiment uses the photon imaging acquisition system (PIAS; Hamamatsu Photonics KK, Japan) that has the active diameter of a photocathode measuring 15 mm with the condition of 1 h 33 min exposure time. To increase the device performance for UPE imaging, a large active area of the photocathode is beneficial. A 2D photon-counting tube with effective diameter of photocathode measuring 40 mm was developed (imaging photon detector, IPD; Photek, UK). It contributed to the success of UPE image of a rat brain *in vivo* [3].

The other type of 2D photon-counting imager system is assembled with an image-intensifier (I.I.) that has the similar configuration to that of the above-described 2D photon-counting tube. It consists of a photocathode, a set of MCPs, and a phosphor screen instead of the position-sensitive anode, in which the image on the photocathode is enhanced on the phosphor screen. The converted image on the phosphor screen is captured using a general imaging device such as a CCD camera or a conventional TV camera via a lens system or a fiber-optic plate. Single photoelectron events shown as bright spots on the phosphor screen are detected using a video-rate camera. They are recorded as counts of photoelectron events to produce a photon-counting image. The schematic configuration of a typical I.I.-based 2D photon-counting imager is presented in Fig. 2, which was assembled with an I.I., a CCD camera, and a fiber-optic plate for image coupling from the phosphor screen to the CCD camera. Camera systems of these types include full forms of the ICCD and IICCD camera.

The UPE images from a germinating soybean seed under intact conditions and injured conditions were reported using an I.I.-based 2D photon-counting imager (video intensified microscope, VIM; Hamamatsu Photonics KK) [4]. The active area of the photocathode was 12 mm diameter; 2500 s exposure time was necessary for this experiment.

The detection limit, defined as the minimum detectable photon-number, is determined by the photocathode quantum efficiency

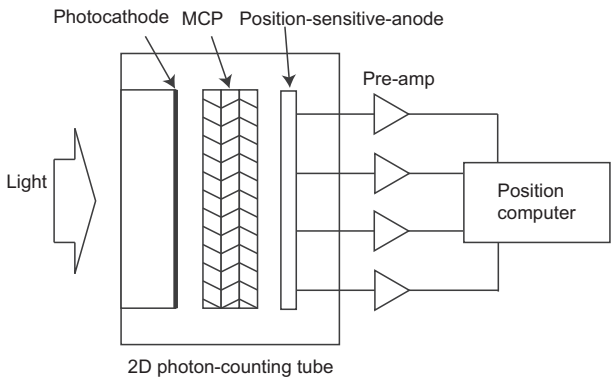

Fig. 1. Schematic diagram of a 2D photon-counting tube.

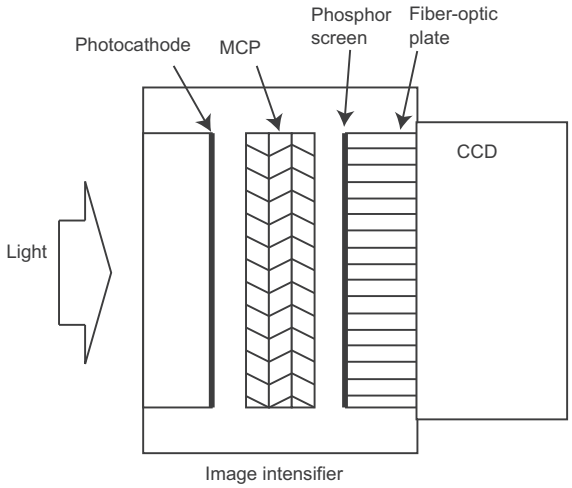

Fig. 2. Schematic diagram of an ICCD camera, as one type of I.I. based 2D photon-counting system.

and the dark current shot noise. In the case in which magnification gain of MCP is sufficient to identify single-photoelectron events, the minimum detectable photon-number is calculable from the equation of signal-to-noise ratio (SNR) represented as presented below.

$$\frac{S}{N} = \frac{\eta\langle N_P\rangle}{\sqrt{\eta\langle N_P\rangle + \langle N_d\rangle}}\sqrt{T} \tag{1}$$

Therein, $\langle N_p\rangle$ and $\langle N_d\rangle$ respectively represent the averaged photon-number and averaged dark counts per pixel in unit time. Here, η and T respectively denote the photocathode quantum efficiency and exposure time for imaging. The minimum detectable photon-number $\langle N_p\rangle_{min}$ is definable under the condition of $S/N = 1$ with $\langle N_p\rangle \ll \langle N_d\rangle$. It is derived as shown below.

$$\langle N_p\rangle_{min} = \frac{1}{\eta}\sqrt{\frac{\langle N_d\rangle}{T}} \tag{2}$$

The 2D photon-counting system provides the benefit of identifying single-photoelectron events in real time, but its spatial resolution is restricted by the performance of the MCP and the position-sensitive-anode, or the resolution of the phosphor screen in the case of an I.I.-based imaging system. The spatial resolution is generally worse than that of the cooled-CCD camera system, as described in the next section.

2.2. Cooled-CCD camera system

CCDs for scientific measurement, which were developed primarily for astronomy, have extremely high sensitivity for ultra-weak light detection. These are also suitable for UPE imaging in the field of biology. The first imaging of UPE of living organisms using a CCD camera (Photometrics, Inc., USA, with Tektronix Inc., CCD) was reported using germinating soybean seedlings [5]. The back-illuminated type, shown as Fig. 3, has excellent sensitivity. Its quantum efficiency at the peak wavelength is close to 90%, even in a cooling condition. Although the CCD has no magnification gain itself, it has better performance for weak light detection than the 2D photon-counting tube described above. That performance is achieved through extension of the integration time and reduction of the amplifier noise (designated as readout noise). The higher quantum efficiency leads to its superiority in terms of performance. For UPE imaging, a large active area for efficient light

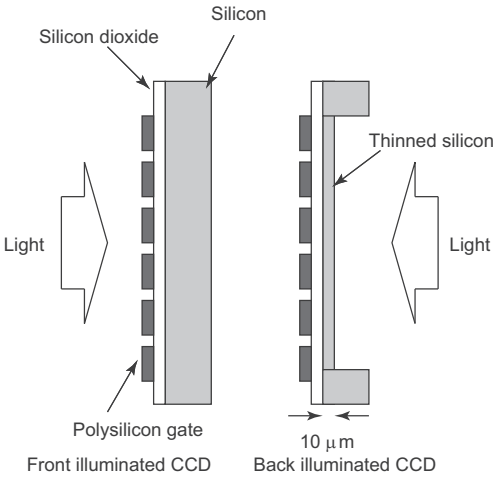

Fig. 3. Schematic illustration of CCD, indicating the difference between front-illuminated type and back-illuminated type.

collection and a back-illuminated structure with full-frame architecture are necessary. Recently, the model CCD42-40 (e2v, UK) is often used for UPE imaging, which has 2048 × 2048 pixel format with the image area measuring 27.6 × 27.6 mm (13.5 μm square pixels).

To reduce dark current, it is necessary to cool the device to about −100 °C. A liquid nitrogen system, a closed-cycle gas cooling system, or a thermo-electronic cooler is usually used. It depends on the features of the camera system provided by some manufacturers.

The SNR for the CCD camera is defined as shown in Eq. (3). Consequently, a minimum detectable photon-number is presented as Eq. (4) under the condition of ultra-weak light measurement.

$$\frac{S}{N} = \frac{\eta\langle N_p\rangle T}{\sqrt{(\eta\langle N_P\rangle + \langle N_d\rangle)T + N_r^2}} \tag{3}$$

$$\langle N_p\rangle_{min} = \frac{1}{\eta}\sqrt{\frac{\langle N_d\rangle}{T} + \frac{N_r^2}{T^2}} = \frac{1}{\eta T}\sqrt{\langle N_d\rangle T + N_r^2} \tag{4}$$

Because the CCD has no-gain, the readout noise, N_r (rms), from the output amplifiers should be regarded as Eq. (3). However, the readout noise can be reduced with low-frequency scanning. With the condition of $\langle N_d\rangle T \gg N_r^2$, which represents long time exposure, the readout noise is negligible. Furthermore, the minimum detectable photon-number $\langle N_p\rangle_{min}$ reaches Eq. (2), similarly to the 2D photon-counting tube. Although it also restricts the time resolution of imaging, it is beneficial for spontaneous UPE, which does not primarily require high-speed imaging.

In practical use, CCD has the function of binning to reduce spatial resolution without degrading SNR, as a tradeoff against the detection limit. The binning operation can increase SNR without the addition of the excess readout noise. This function is extremely important for UPE imaging because, if the reduction of spatial resolution is conducted by software after full-format readout (software binning), it causes the addition of excess readout noise, thereby degrading the SNR.

Recently, electron multiplying CCD (EMCCD), which comprises an ion-impacted gain process as a gain resistor is inserted between a readout amplifier and a serial resistor, has become widely used for the application of highly sensitive imaging in the field of life sciences. It provides the benefit that readout noise can be ignored because the signal is multiplied with the gain of the factor of a few thousand, offering high-speed imaging of weak light. However, the gain process accompanies the additional noise originating from the statistical fluctuation of the gain. The SNR is derived as shown in Eq. (5).

$$\frac{S}{N} = \frac{\eta\langle N_p\rangle MT}{\sqrt{(\eta\langle N_P\rangle + \langle N_d\rangle)F^2M^2T + N_r^2}} = \frac{\eta\langle N_p\rangle\sqrt{T}}{\sqrt{(\eta\langle N_P\rangle + \langle N_d\rangle)F^2 + N_r^2/M^2T}} \tag{5}$$

Here, M is the gain; F is the excess noise factor representing the fluctuation of the gain. Then the minimum detectable photon-number $\langle N_p\rangle_{min}$ is expressed as Eq. (6). Even under the condition of long time exposure, $\langle N_d\rangle T\ M^2 \gg N_r^2$, it is deduced to Eq. (7), indicating worse performance than that of CCD in the same condition as expressed as Eq. (2). In general, excess noise factor F is known to depend on the gain M, as in the condition of $M > 20$, $F^2 \cong 2$, meaning that the minimum detectable photon-number in EMCCD is worse than CCD with the factor of $\sqrt{2}$ [6].

$$\langle N_p\rangle_{min} = \frac{1}{\eta}\sqrt{\frac{\langle N_d\rangle F^2}{T} + \frac{N_r^2}{M^2T^2}} = \frac{1}{\eta T\ M}\sqrt{\langle N_d\rangle TF^2M^2 + N_r^2} \tag{6}$$

$$\langle N_p\rangle_{min} = \frac{F}{\eta}\sqrt{\frac{\langle N_d\rangle}{T}} \tag{7}$$

Consequently, for spontaneous UPE imaging, which requires long time exposure, CCD is superior to EMCCD. However, in the future, if single photoelectron detection, i.e. real photon-counting, was achieved by EMCCD camera, similar to silicon PMTs which are operated in Geiger-mode with high detection efficiency, then it will be the best solution for UPE imaging.

2.3. Lens system

Adoption of a lens system is crucial for UPE imaging. Particularly, the throughput of the lens system, determined by the f number (or numerical aperture: NA) and total optical transmittance of lens elements, should be assigned top priority. Commercially available lens systems are designed to assign priority to the performance of resolution determined by various aberrations. However, spontaneous emission of UPE inherently cannot require higher spatial resolution because of its weak intensity. Therefore, the lens system is recommended to be designed with priority on throughput under the optimum condition with specific magnification for experimental targets. In previously reported UPE imaging experiments, a commercially available higher throughput lens system; Nikkor 50 mm f/1.2 (Nikon Corp., Japan) was commonly used. Otherwise, a tandem configuration of two pieces of Nikkor f/1.2 lens or a converted Nikkor f/1.2 lens with enlargement of the aperture to avoid vignetting was used. Here, the f number is defined as the ratio of the focal length to the aperture diameter. In commercial lens systems, the nominal f number is defined under the condition of the object distance in infinity. In the practical condition of UPE imaging, the light collection efficiency determined by the solid-angle to the lens system from the object is less than the efficiency suspected from the nominal f number of the commercial lens system. However, in a specifically designed lens system for UPE, the f number can be designed as the practical condition for imaging, not infinity. Besides, minimization of the number of elements in the lens system also achieves marked improvement of throughput. Consequently, the lens system throughput is more than double that of the commercially available lens system. In a report about *in vivo* rat brain imaging, a specially designed lens system providing 0.45 NA at magnification of 1.0 was used [7]. The lens system comprised six lenses,

Table 1
Notable reports of UPE imaging targeting spontaneous emission from living organisms.

Sample	Condition	Imaging device	Exposure time	Lens system	Author (Affiriation)	Year
Soybean seedling	Intact	2D PMT (PIAS, HPK)	93 min	Nikkor 50 mm *f*/1.2	Scott, Inaba (Inaba Biophoton Proj.)	1989 [2]
Soybean seedling	Intact	2D PMT (PIAS, HPK)	120 min	Nikkor 50 mm *f*/1.2	Ichimura, Hiramatsu (HPK)	1989 [8]
Soybean seeding/Azuki bean	Injured (intact)	I.I. (VIM/ARGUS, HPK)	42 min / 60 min		Suzuki, Inaba (Inaba Biophoton Proj.)	1991 [4]
Cucumber seedling	Intact/injured	2D PMT (PIAS, HPK)	19 min	Nikkor 50 mm *f*/1.2	Schauf, Kaufmann (Dusseldorf Univ.)	1992 [9]
Red bean seedling	Intact	2D PMT (PIAS, HPK)			Kai (Kyushu Univ.)	1994 [10]
Fungi infected sweet potato	Infection	I.I. (VIM/ARGUS, HPK)	5 min		Makino (Shizuoka Agr. Exp. Sta.), Hiramatsu (HPK)	1995 [11]
Cancer bearing mouse	Intact	I.I. (VIM/ARGUS, HPK)	120 min	*f*/0.82 (infinity)	Amano (Kanazawa Univ.), Inaba (Inaba Biophoton Proj.)	1996 [14]
Soybean seedling	Intact/injured	Cooled CCD (ATC200C, Photometrix/CCD: TK1024, Tektronix)	30 min (2×2 binning)	Nikkor *f*/1.2 tandem	Kobayashi, Inaba (Biophotonics Inf. Lab.)	1997 [5]
Rat brain	Intact	2D PMT (IPD, Photek)	60 min	Special design NA/0.45	Kobayashi, Inaba (Biophotonics Inf. Lab.)	1999 [3,7]
Cancer bearing mouse	Intact	Cooled CCD (ATC200C, Photometrix/CCD:TK1024, Tektronix)	60 min (2×2 binning)	Nikkor 50 mm *f*/1.2	Takeda, Inaba (Biophotonics Inf. Lab.)	2004 [15]
Virus infected leaf	Infection	Cooled CCD (ORCA II, HPK)	15 min (2×2 binning)	Nikkor 35 mm *f*/2.8	Bennet (Imp. Col. London)	2005 [12]
Human body	Intact	Cooled CCD (600S, Spectral Instr./CCD42-40, e2v)	30 min (8×8 binning)	Special design	Van Wijk (Utrecht Univ.), Kobayashi (Tohoku Inst. Tech.)	2006 [16]
Virus infected leaf	Infection	2D PMT (IPD, Photek)	120 min	Special design NA/0.5	Kobayashi (Tohoku Inst. Tech.)	2007 [13]
Human body	Intact	Cooled CCD (600S, Spectral Instr./CCD42-40, e2v)	60 min 20 min (8×8 binning)	Special design NA/0.5	Kobayashi (Tohoku Inst. Tech.)	2009 [17]
Human hand	Intact	Cooled CCD (VersArray 1300B, Princeton Instr./CCD36-40, e2v)	30 min (4×4 binning)	Nikkor 50 mm *f*/1.2	Prasad, Pospisil (Palacky Univ.)	2011 [18,19]

Abbreviations: 2D PMT: two-dimensional photon-counting tube, HPK: Hamamatsu Photonics KK.

with relative illuminance on the lens system at an image height of 50% from the light axis designed to reach more than 88% on the axis for improvement of the throughput. Results show that the spatial resolution of the lens system was confined for approximately 5 line-pairs/mm to provide a superior *NA* [7].

3. Application of UPE imaging

Next, we present a review of UPE imaging experiments to observe spontaneous emissions from living organisms. Some notable reports describing UPE imaging with comparison from technical features are presented in Table 1. Along with the development of 2D photon-counting technique, at the end of the 1980s, the first observations of UPE images were achieved using plant materials. As described above, germinating seeds and roots were samples that were reported initially [2,4,5,8–10]. These experiments suggest the feasibility of imaging to identify physiological information through localization of active areas. Furthermore, temporal changes of UPE images, those which reflect biological responses induced by stress of various kinds such as injury or infection were explored. As applications characterizing defensive responses to infection, the emission patterns of UPE induced by fungi on sweet potatoes [11] and specific UPE images induced with various viral infections on plant leaves [12,13] accompanied by temporal changes were reported. These were demonstrated and discussed as ROS-associated physiological responses, suggesting the feasibility of application for non-invasive and quantitative monitoring of plant resistance to infection. The value of UPE in this process is suspected to originate in the production of ROS and/or ROS or other molecules mediating physiological reaction. Designated as the hypersensitive response, it is induced by the recognition of resistant proteins as a trigger of plant defense mechanisms before the occurrence of localized cell death.

The UPE imaging of small animals requires long-term exposure. It then requires anesthesia during measurement. Instruments to maintain body conditions of the animals and preparation with hair removal or the use of hairless mice are necessary with careful treatment of animals. Regarding feeding, the feed should be chosen carefully so that it does not contain fluorescent materials because the contents of feed affect photon emissions from the body inside as background emissions. Experiments of UPE imaging of a rat brain observed through the skull [3] or with partial removal of the skull [7] have been reported. An earlier report described the feasibility of imaging of UPE on the surface of rat brain through the skull with demonstration of the correlation between UPE intensity and electroencephalographic activity. Results of UPE experiments using brain slices suggest that the UPE reflects the energy metabolism associated with ROS production in the mitochondrial electron transfer chain. Furthermore, whole body imaging of cancer-bearing nude mice [14,15] was reported, demonstrating UPE changes with indication of the correlation between UPE intensity and the tumor growth rate, which offers quantitative information related to tumor malignancy [15].

The human body is an attractive target of UPE imaging for applications aimed at diagnosis. Skin health or the holistic state of the body condition representing metabolic activity is expected to be visualized. UPE imaging of the human skin surface reveals specific patterns of photon emissions [16–19]. Practical applications assessing the oxidative stress of skin have been explored through topical application of ROS or their scavengers, or ultraviolet (UV) irradiation [18,19]. On the other hand, as an indicator of holistic states of living body, changes of emission intensity corresponding to diurnal variation have been reported [17].

The most important shortcoming of UPE imaging for practical application is its requirement of long exposure. For the imaging of animals and humans, exposure times should be more than 10 min to 1 h. An important implication is that the effects of background emissions derived from auto-fluorescence and/or delayed luminescence are not negligible in measurements. These must be treated carefully to avoid affecting the UPE signals. Strict measurement procedures such as dark adaptation and careful preparation of washing or cleaning can provide reliable and precise images, suggesting that some protocol of measurement for standardization of UPE imaging is necessary. However, the obscurity of complex mechanisms and the difficulty of determining emission species on UPE also make it difficult for use in practical applications.

4. Conclusion

Imaging technology of UPE, spontaneously emitted from living organisms, was reviewed along with imaging experiments for developing applications in medical and agricultural fields. UPE imaging has great potential for non-invasive monitoring as a completely passive method, thereby offering an 'ultimate' methodology for diagnosis. Historical aspects of achievements and technical constraints of UPE imaging were also described.

To develop and accomplish the practical application of UPE, improvement of performance with shortening of the exposure time for imaging might be necessary. However, the quantum efficiency of CCD is close to 90%. Throughput of the lens system for UPE imaging reaches the limitations from the design concept described above. Now the overall efficiency of photon detection of the imaging system is apparently near the physical limit, implying the necessity of developing a novel methodology for UPE utilization. For example, adaptively valuable resolution of UPE imaging and/or addition of spectral information related to spatial data to extract specific properties of UPE are anticipated. Moreover, improvement of spectroscopic techniques and the advancement of a spectral database including putative emission mechanisms and species are necessary. Spatial data associated with simultaneously measured spectral information might overcome the shortcomings of UPE imaging. Pursuit of a breakthrough in the measurement and analysis of UPE might yield actual non-invasive tools for use in future diagnoses.

5. Abbreviations

UPE	ultra-weak photon emission
ROS	reactive oxygen species
2D	two-dimensional
CCD	charge-coupled-device
MCP	micro-channel plates
I.I.	image-intensifier
SNR	signal-to-noise ratio
EMCCD	electron multiplying CCD
UV	ultraviolet

References

[1] Y. Tuchiya, E. Inuzuka, T. Kurono, M. Hosoda, Photon-counting imaging and its application, Adv. Electron. Electron. Phys. 64A (1985) 21–31.
[2] R.Q. Scott, M. Usa, H. Inaba, Ultraweak emission imagery of mitosing soybeans, Appl. Phys. B 48 (1989) 183–185.
[3] M. Kobayashi, M. Takeda, T. Sato, Y. Yamazaki, K. Kaneko, K.-I. Ito, H. Kato, H. Inaba, In vivo imaging of spontaneous ultraweak photon emission from a rat's brain correlated with cerebral energy metabolism and oxidative stress, Neurosci. Res. 34 (1999) 103–113.
[4] S. Suzuki, M. Usa, T. Nagoshi, M. Kobayashi, N. Watanabe, H. Watanabe, H. Inaba, Two-dimensional imaging and counting of ultraweak emission patterns from injured plant seedlings, J. Photochem. Photobiol. B 9 (1991) 211–217.
[5] M. Kobayashi, B. Devaraj, M. Usa, Y. Tanno, M. Takeda, H. Inaba, Two-dimensional imaging of ultraweak photon emission from germinating soybean seedlings with a highly sensitive CCD camera, Photochem. Photobiol. 65 (1997) 535–537.
[6] M. Robbins, B. Hadwen, The noise performance of electron multiplying charge-coupled devices, IEEE Trans. Electron. Dev. 50 (2003) 1227–1232.
[7] M. Kobayashi, M. Takeda, T. Sato, Y. Yamazaki, K. Kaneko, K.-I. Ito, H. Kato, H. Inaba, Two-dimensional photon counting imaging and spatiotemporal characterization of ultraweak photon emission from a rat's brain in vivo, J. Neurosci. Method 93 (1999) 163–168.
[8] T. Ichimura, M. Hiramatsu, N. Hirai, T. Hayakawa, Two-dimensional imaging of ultra-weak emission from intact soybean roots, Photochem. Photobiol. 50 (1989) 283–286.
[9] B. Schauf, L.M. Repas, R. Kaufmann, Localization of ultraweak photon emission in plants, Photochem. Photobiol. 55 (1992) 287–291.
[10] S. Kai, T. Mitani, M. Fijikawa, Morphogenesis and bioluminescence in germination of red bean, Physica A 210 (1994) 391–402.
[11] T. Makino, K. Kato, H. Lyozumi1, H. Honzawa, Y. Tachiiri, M. Hiramatsu, Ultraweak Luminescence generated by sweet potato and fusarium oxysporum interactions associated with a defense response, Photochem. Photobiol. 64 (1996) 953–956.
[12] M. Bennett, M. Mehta, M. Grant, Biophoton imaging: a nondestructive method for assaying R gene responses, MPMI 18 (2005) 95–102.
[13] M. Kobayashi, K. Sasaki, M. Enomoto, Y. Ehara, Highly sensitive determination of transient generation of biophotons during hypersensitive response to cucumber mosaic virus in cowpea, J. Exp. Bot. 58 (2007) 465–472.
[14] T. Amano, M. Kobayashi, B. Devaraj, M. Usa, H. Inaba, Ultraweak biophoton emission imaging of transplanted bladder cancer, Urol. Res. 23 (1995) 315–318.
[15] M. Takeda, M. Kobayashi, M. Takayama, S. Suzuki, T. Ishida, K. Ohnuki, T. Moriya, N. Ohuchi, Biophoton detection as a novel technique for cancer imaging, Cancer Sci. 95 (2004) 656–661.
[16] R. van Wijk, M. Kobayashi, E. van Wijk, Anatomic characterization of human ultra-weak photon emission with a movable photomultiplier and CCD imaging, J. Photochem. Photobiol. B 83 (2006) 69–76.
[17] M. Kobayashi, D. Kikuchi, H. Okamura, Imaging of ultraweak spontaneous photon emission from human body displaying diurnal rhythm, PLoS ONE 4 (2009) e6256.
[18] A. Prasad, P. Pospišil, Two-dimensional imaging of spontaneous ultraweak photon emission from the human skin: role of reactive oxygen species, J. Biophoton. 4 (2011) 840–849.
[19] A. Rastogi, P. Pospišil, Spontaneous ultraweak photon emission imaging of oxidative metabolic processes in human skin: effect of molecular oxygen and antioxidant defense system, J. Biomed. Opt. 16 (2011) 096005.